Published in final edited form as:

Nat Med. 2014 October ; 20(10): 1174–1181. doi:10.1038/nm.3655.

Inhibition of JAK/STAT signaling stimulates adult satellite cell function

Feodor D. Price[1,2,5], **Julia von Maltzahn**[1,2,4,5], **C. Florian Bentzinger**[1,2], **Nicolas A. Dumont**[1,2], **Hang Yin**[1,2], **Natasha C. Chang**[1,2], **David H. Wilson**[1], **Jérôme Frenette**[3], and **Michael A. Rudnicki**[1,2,6]

[1]Sprott Center For Stem Cell Research, Ottawa Hospital Research Institute, Regenerative Medicine Program, 501 Smyth Road, Ottawa, ON, Canada, K1H 8L6

[2]University of Ottawa, Cellular and Molecular Medicine, Faculty of Medicine, 501 Smyth Road, Ottawa, ON, Canada, K1H 8L6

[3]CHUQ-CRCHUL, 2705 Blvd. Laurier, T-R-93, Sainte-Foy, QC, Canada, G1V 4G2

Abstract

Diminished regenerative capacity of skeletal muscle occurs during adulthood. We identified a reduction in the intrinsic capacity of murine adult satellite cells to contribute to regeneration and repopulate the niche. Gene expression analysis identified an increase in expression of JAK/STAT signaling targets between 3 week old and 18 month old mice. Knockdown of Jak2 or Stat3 significantly stimulated symmetric satellite stem cell divisions on cultured myofibers. Knockdown of Jak2 or Stat3 in prospectively isolated satellite cells markedly enhanced their ability to repopulate the satellite cell niche. Pharmacological inhibition of Jak2 and Stat3 similarly stimulated symmetric expansion of satellite cells *in vitro* and their engraftment *in vivo*. Intramuscular injection of these drugs resulted in a dramatic enhancement of muscle repair and force generation. Together these results reveal intrinsic properties that functionally distinguish adult satellite cells and suggest a promising therapeutic avenue for the treatment of muscle wasting diseases.

Keywords

Skeletal muscle; satellite cell; stem cells; aging; JAK/STAT signaling

[6]Correspondence should be addressed to M.A.R., Tel: (613) 739-6740, Fax: (613) 739-6294, mrudnicki@ohri.ca.
[4]Current address: Fritz-Lipmann Institute for Age Research, Beutenbergstrasse 11, 07745 Jena, Germany
[5]These authors contributed equally to this work

COMPETING FINANCIAL INTERESTS

The authors declare no competing financial interests.

INTRODUCTION

The growth, maintenance, and regeneration of skeletal muscle is attributed to the satellite cell; a mitotically quiescent stem cell that resides between the basal lamina and sarcolemma of the muscle fiber[1–3]. Satellite cells can self-renew and it is this characteristic that allows adult skeletal muscle to undergo multiple rounds of regeneration[4–6]. The functional and structural decline of skeletal muscle in adulthood is one of the first hallmarks of aging in many organisms[7–9]. Intriguingly, as an organism ages a decrease in skeletal muscle function is concomitant with a decrease in satellite cell numbers[10,11].

The reduced regenerative potential observed in ageing skeletal muscle is primarily attributed to changes in the muscle niche. Soluble ligands from the Notch, Wnt and TGF-β signaling pathways are deregulated both systemically and within the satellite cell niche[12–15]. Alterations in the activity of these pathways in combination with fibrosis and an increased immune response result in age related deficiencies in satellite cell self-renewal and regenerative efficacy[16]. Notably, a recent publication describes intrinsic changes in geriatric satellite cells involving de-repression of p16 (Ink4a) in mice over 28 months of age[17]. Other recent studies implicate the p38α and p38β mitogen-activated kinase pathway in the age related intrinsic changes that occur in aged satellite cells from mice[18–20]. Moreover, differences in satellite cell number and proliferative capacity are noted in mouse and rat satellite cells isolated from 3 month versus 7 month old skeletal muscle[11,21,22]. Taken together, these findings indicate that age-related changes in satellite cell self-renewal, proliferative and differentiation capacity are likely due to both extrinsic alterations in the microenvironment and to intrinsic alterations in cell-autonomous regulatory mechanisms.

To identify age-related intrinsic functional differences in satellite cells, we examined the transcriptional profile and regenerative capacity of satellite cells isolated from mice at different ages. We identified a role for JAK/STAT signaling in mediating this decline by impairing satellite cell function through the stimulation of asymmetric division.

RESULTS

Adult satellite cells exhibit decreased engraftment

To further characterize the intrinsic functional differences in satellite cells as they progress through adulthood, we isolated 3 week (adolescent), 2–4 month (young adult) and 18 ± 2 months (older adult) satellite cells by fluorescence activated cell sorting (FACS) from *Pax7-ZsGreen* reporter mice[23] (Supplementary Fig. 1a). We observed that with increasing age, satellite cells decrease in number, express higher levels of ZsGreen/Pax7 and alter their cell surface complement (Supplementary Fig. 1b–d).

To investigate whether satellite cells intrinsically differ with age in their functional capacity to participate in muscle regeneration, we transplanted 10,000 freshly sorted *Pax7-ZsGreen* expressing satellite cells from mice of different ages into regenerating TA muscle of 6–8 week old immunosuppressed *mdx* mice (Fig. 1a). Muscles from recipient *mdx* mice transplanted with wild type satellite cells from older adult mice displayed a ~2-fold decrease (53% ± 14%) in the percentage of dystrophin expressing myofibers relative to recipients

who were transplanted with young adult satellite cells (100% ± 21%), while recipients of adolescent satellite cells displayed a ~2-fold increase (144% ± 19%) (Fig. 1b,c and Supplementary Fig. 2b,c).

We also enumerated the number of donor-derived cells that engraft as satellite cells. Isolated TA muscle sections were stained for ZsGreen to quantify transplanted cells and Pax7/DAPI to confirm their continued satellite cell identity (Fig. 1d,e and Supplementary Fig. 2c,d,e). Transplanted satellite cells from older adult donors displayed a ~3-fold reduction in their ability to contribute to the satellite cell pool relative to young adult and adolescent cells (older adult 34% ±5%, young adult 100%, and adolescent 113% ±10%).

Pathway analysis identifies an age-related activation of JAK/STAT signaling

To investigate how age governs the transcriptional profile of satellite cells, we performed a genome wide expression analysis on freshly sorted satellite cells from mice of different ages (adolescent, n=3, pooled group of 6; young adult, n=3, pooled group of 8; and older adult, n=3, pooled group of 8). Pearson correlation along with principle component analysis (PCA) conducted between the three satellite cell populations and proliferating myoblasts clustered all satellite cell populations as distinct and significantly different from primary myoblasts (Supplementary Fig. 3a,b).

We next conducted an unbiased DAVID analysis of the satellite cell microarray data across each age group. GO term analysis of genes up regulated (>2-fold) in adolescent relative to older adult *ZsGreen*-expressing cells identified broad categories of cell cycle regulation, cell division, chromatin organization, and striated muscle development (Supplementary Fig. 3c). By contrast, GO term analysis conducted on genes up regulated (>2-fold) in older adults relative to adolescent satellite cells demonstrated enrichment for immune response, vascular development, oxidation reduction and regulation of apoptosis (Supplementary Fig. 3d).

To identify signaling pathways that are differentially activated in adult satellite cells we conducted Gene Set Enrichment Analysis (GSEA) between our adolescent and older adult satellite cell data sets[24]. RMA normalized gene sets for adolescent and older adult satellite cells were analyzed based on the Kyoto encyclopedia of genes and genomes (KEGG) suite in GSEA to identify enriched signaling pathways. Following GSEA KEGG analysis we selected the most significantly enriched signaling pathways based on their normalized enrichment score (NES) (Fig. 2a and Supplementary Fig. 3e). Several of the enriched KEGG signaling pathways in older adult satellite cells have been linked directly to satellite cell function including Notch signaling[14,25], Janus associated kinase-signal transducer and activator of transcription JAK/STAT signaling[26], Transforming growth factor β signaling (TGF-β)[13] and MAPK signaling[27].

To further identify the important signaling pathways involved we conducted motif analysis in GSEA to identify transcription factor binding sites present in the promoters of genes enriched in older adult relative to adolescent satellite cells. Notably, within older adult gene promoters, the enrichment (NES > 1.2) of binding sites for STATs, STAT co-activators and activators of JAK/STAT signaling was the most significant (Supplementary Table 1a).

To confirm the enrichment in expression of genes involved in JAK/STAT signaling with increasing age, we generated global ratio heat maps based on the fold change relative to adolescent Log2 transformed RMA values from our microarray data sets (Fig. 2b and Supplementary Fig. 4). Genes involved in JAK/STAT signaling whose expression increased significantly with respect to age were validated by qPCR analysis on freshly sorted satellite cells from mice of different ages (Fig. 2c). We observed strong upregulation of the JAK/STAT targets *Socs3* (9-Fold), *Bcl2* (5-fold), *Bcl6* (5-fold), *Pim1* (4-fold) and *Myc* (3.5-fold) in older adult relative to young adult or adolescent satellite cells (Fig. 2c). Furthermore, we similarly observed statistically significant increases in the JAK/STAT co-activators JunD (30-fold) and Cebpd (32-fold), and Fos (13-fold) along with activators of JAK/STAT signaling EGFR (3.5-fold), AR (3.5-fold) and Gp130 (2 fold) in older adult relative to young adult or adolescent satellite cells (Fig. 2c).

To validate the increase in JAK/STAT expression with age we quantified the amount of Stat3 phosphorylated on tyrosine 705 (p-Stat3) from freshly sorted satellite cells using microcapillary isoelectric focusing. Notably, p-Stat3 proteins levels increased ~1.6-fold (young adult) and 2.4-fold (older adult) with respect to adolescent satellite cells (Fig. 2d and Supplementary Fig. 3f).

Inhibition of JAK/STAT signaling promotes symmetric expansion

To investigate the role of JAK/STAT signaling in satellite cell activation and commitment, we cultured isolated single myofibers for 42h or 72h with siRNAs targeting either Jak2 or Stat3. Consistent with our FACS analysis, enumeration of the numbers of satellite cells per myofiber revealed that the average satellite cell number per myofiber prior to *in vitro* culture decreased with age by ~1.6-fold from 2.1 ± 0.39 (young adult) to 1.2 ± 0.16 (older adult) and a further 2.6-fold when comparing adolescent (3.2 ± 0.79) to older adult (Supplementary Fig. 5a,b).

Satellite stem cells represent a subpopulation of satellite cells that are capable of long-term self-renewal and repopulation of the satellite cell niche following transplantation[5]. Cre-LoxP mediated lineage tracing using *Myf5-Cre* and *R26R-YFP* alleles allows the discrimination between committed satellite myogenic cells that have expressed *Myf5-Cre* (YFP^+), and the subpopulation (<10%) of satellite stem cells that have never expressed *Myf5-Cre* (YFP^-)[5]. Satellite stem cells can undergo either planar symmetric divisions to give rise to two stem cells, where the orientation of the division is parallel to the basal lamina, or alternatively undergo an apical-basal asymmetric division to give rise to a stem cell and a committed cell, where the orientation of the division is at a right angle to the basal lamina.

To investigate whether inhibition of JAK/STAT signaling would promote the symmetric expansion of satellite stem cells, we treated single myofibers isolated from young adult mice for 42h *ex vivo* with siRNAs against Stat3, Jak2 or a scrambled control and assessed the number of cell doublets and whether or not they occurred in a symmetric or asymmetric fashion. Treatment with siStat3 and siJak2 significantly promoted symmetric satellite cell divisions (Fig. 3a) ~2-fold while having no significant effect on the overall number of dividing satellite cells after 42h of culture relative to vehicle treated controls (Fig. 3b). To investigate whether this effect is maintained in older adult skeletal muscle we examined the

ability of siJak2 and siStat3 to promote planar satellite cell divisions on single myofibers from 18-month-old mice. Myofibers treated with siStat3 display an ~2.8 fold increase, while siJak2 treated myofibers display an ~2.6 fold increase in the number of planar divisions relative to vehicle controls after 42 h in culture (Supplementary Fig. 5d).

Satellite cells activate from quiescence following muscle injury and initiate the expression of the transcription factor MyoD. Expression of MyoD is associated with acquisition of progenitor status, and subsequent down regulation of Pax7 ($Pax7^{-}/MyoD^{+}$) is followed by differentiation[11,29–31]. The average number of $Pax7^{+}$ cells per myofiber, after 72h of culture, was ~15% more in adolescent mice following treatment with siStat3 (Fig. 3c), and ~26% more following siJak2 treatment in myofibers from young adult mice. The percentage of $Pax7^{-}/MyoD^{+}$ satellite cells undergoing differentiation was lower following siStat3 (~8% (adolescent) and ~76% (young adult)) or Jak2 (~24% (adolescent) and ~74% (young adult)) (Fig. 3d).

We also treated single myofibers *ex vivo* with inhibitors of the JAK/STAT signaling pathway (Jak2 - Tyrphostin AG 490; and Stat3 – 5, 15 DPP)[28–30]. Notably, treatment with these inhibitors significantly promoted symmetric satellite cell divisions (Fig. 3e) while having no significant effect on the overall number of dividing satellite cells after 42h of culture (Fig. 3f).

Following treatment with inhibitors of JAK/STAT signaling for 72h we observed a statistically significant increase in the average number of young adult $Pax7^{+}$ satellite cells/myofiber in both 5, 15 DPP (40 ± 5) and Tyrphostin AG 490 (31 ± 3) treated samples (Fig. 3g and Supplementary Fig. 5c). Inhibition of JAK/STAT signaling had a marginal effect on the numbers of satellite cells on myofibers isolated from adolescent mice. Likewise, we observed an increase in the average number of older adult Pax7-expressing satellite cells/myofiber following treatment with 5, 15 DPP (27 ± 3), or Tyrphostin AG 490 (29 ± 3) relative to our vehicle control (15 ± 3) (Fig. 3g and Supplementary Fig. 5c). Isolated 18-month-old myofibers cultured for 42h displayed an increase in the number of planar satellite cell divisions (5, 15 DPP, ~2.0-fold increase; Tyrphostin AG 490, ~2.3-fold increase; combination of 5, 15 DPP + Tyrphostin AG 490, ~1.7-fold increase) (Supplementary Fig. 5e). Following JAK/STAT inhibitor treatment, the percentage of $Pax7^{-}/MyoD^{+}$ cells was decreased in young adult (~30% on average) and to an even greater extent in older adult (~50% on average) following treatment with JAK/STAT inhibitors (Fig. 3h).

Reduction of Jak2 or Stat3 enhances engraftment

We employed FACS to isolate quiescent *Pax7-ZsGreen* satellite cells from 3 month old mice, transfected them *ex vivo* for 3 h on ice with siStat3 and/or siJak2 followed by transplantation into the TA muscle of wild type (C57Bl/6) mice that had been injured with cardiotoxin (CTX) 2 days prior (Fig. 4a). Twelve days after transplantation, mice were sacrificed and the engraftment of Pax7 and ZsGreen double-positive ($Pax7^{+}/ZsGreen^{+}$) cells was assessed (Fig. 4b). Knockdown of Stat3 resulted in an ~80% increase in the repopulating capacity (from 55% ± 10 in the siSTAT3 condition compared to ~31% ± 4% in the siScrambled control) (Fig. 4c and Supplementary Fig. 6). Likewise, the inhibition of

Jak2 (54% ± 7%) or the simultaneous inhibition of both Stat3 and Jak2 (49% ± 7%) resulted in an ~80% and a ~58% increase respectively (Fig. 4d).

To further assess the potential for clinical application of pharmacological inhibition of JAK/STAT signaling, we treated satellite cells from young adult and older adult mice with drug inhibitors to determine their effect on engraftment potential (Fig. 5a and Supplementary Fig. 7a).

Satellite cells from 3-month-old mice treated with 5,15 DPP or Tyrphostin AG 490 for 3h post isolation displayed an increased ability of 100% ± 16% and 85% ± 30% to engraft respectively relative to vehicle controls (Fig. 5b). Treatment of satellite cells from older adult mice with 5,15 DPP or Tyrphostin AG 490 further improved engraftment by 126% ± 37% and 125% ± 17% respectively (Fig. 5b), while no increase in the number of resident satellite cells was observed following transplantation (Supplementary Fig. 7b).

To validate these results in a disease model, we conducted similar experiments using *mdx* mice as recipients. Following treatment of satellite cells from young adult and older adult mice with JAK/STAT inhibitors, we observed a statistically significant increase in the percentage of donor ($ZsGreen^+$) satellite cells relative to vehicle treated controls (Fig. 5c).

We performed a serial injury experiment to ensure that the transplanted $ZsGreen^+$ cells were *bona fide* satellite cells capable of self-renewal (Supplementary Fig. 7c). We observed a similar percentage of donor derived $Pax7^+/ZsGreen^+$ following re-injury providing conclusive evidence that the transplanted cells were indeed *bona fide* satellite cells capable of self-renewal (Supplementary Fig. 7d).

Injection of JAK/STAT inhibitors enhances repair

Our experiments raise the possibility that pharmacological inhibition of JAK/STAT signaling *in vivo* represents a potential therapeutic approach to stimulate muscle regeneration. Therefore, we injured the TA muscle of young adult and older adult C57BL/6 mice with cardiotoxin (CTX) to initiate regeneration followed by direct intramuscular (IM) injection of JAK/STAT pathway inhibitors (Fig. 6a). We observed an increase in the minimal fiber feret[31] in either young adult or older adult skeletal muscle following IM injection of JAK/STAT inhibitors (Fig. 6b and Supplementary Fig. 8a). We also observed a decrease in the number of $devMyHC^+$ fibers in young adult and older adult muscle treated with JAK/STAT signaling inhibitors (Supplementary Fig. 8b). This reduction in the number of devMyHC positive myofibers was increased in older adult muscle, where the proportion of devMyHC myofibers decreased from 83% ± 10% (vehicle) to 48% ± 7.3% (5,15 DPP), 40% ± 12% (Tyr AG 490), and 30% ± 8.2% (5,15 DPP + Tyr AG 490) respectively (Supplementary Fig. 8b).

We examined macrophage infiltration (CD11b), connective tissue formation (Sirius Red) and general muscle architecture (H&E stain). Injection of JAK/STAT inhibitors resulted in a decrease in macrophage infiltration (Supplementary Fig. 9a), reduced Sirius Red staining, and improved in muscle architecture as evidenced by H&E staining (Supplementary Fig. 9b,c).

We found an increase of ~50% (young adult) or ~100% (older adult) in the total number of satellite cells (Fig. 6c) as well as the number of satellite cells that do not express MyoD ($Pax7^+/MyoD^-$) (Supplementary Fig. 8c). Furthermore we observed an increase in the proportion of satellite cells that lack MyoD expression ($Pax7^+/MyoD^-$) following treatment (Supplementary Fig. 8d).

To address whether JAK/STAT inhibition functionally improves the performance of damaged skeletal muscle, we injured the extensor digitorum longis (EDL) muscle from young adult mice with CTX followed by IM injection of JAK/STAT inhibitors 3 d after injury (Fig. 6f). Treatment with JAK/STAT inhibitors significantly increased the peak force observed over time (Fig. 6g). Under control conditions the maximal force of regenerating EDL muscle measured was 11.3 ± 0.8 N/cm2. Notably, following IM injection of JAK/STAT inhibitors the maximal force of EDL muscle improved to 11.8 ± 0.5 N/cm2 (5,15 DPP), 12.7 ± 1.3 N/cm2 (Tyr AG 490) and 14.2 ± 0.7 N/cm2 (5,15 DPP + Tyr AG 490) respectively (Fig. 6h). Furthermore, treatment with JAK/STAT inhibitors decreased the rate of reduction of muscle force over time observed in fatigue tests (Fig. 6i).

DISCUSSION

Changes in the microenvironment and other extrinsic factors are thought to be the major cause of the progressive decline in skeletal muscle regenerative capacity throughout adulthood[14,16,25]. However, de-repression of p16 (Ink4a) has been shown to intrinsically shift satellite cells into deep quiescence in mice over 28 months of age[17]. In addition, over activation of p38α and p38β mitogen-activated kinase pathway also contributes to diminished function in satellite cells from aged (24 month) mice[18–20]. Therefore, satellite cells undergo profound cell autonomous alterations, potentially as a result of changes to their microenvironment, that result in altered functional capacity even after transplantation into a young environment. Our results suggest that intrinsic changes in satellite cell functional capacity begin at a much younger age.

Our data suggests that one distinguishing feature of satellite cells as they age is the concerted activation of JAK/STAT pathway. Known activators of JAK/STAT signaling include LIF, bFGF, IL6, PDGF, EGF and androgen[32,33]. The JAK/STAT signaling pathway is involved in skeletal muscle differentiation whereby Stat3 activation mediated by extracellular interleukins (IL6, LIF) affects MyoD and promotes myoblast differentiation[34]. Furthermore, previous reports demonstrate activation of the (JAK/STAT) signaling pathway in satellite cells of aged human skeletal muscle[35]. JAK/STAT signaling pathway members include suppressor of cytokine signaling 3 (*Socs3*), *c-Myc*, *Fos*, *JunB*, *CEBPδ* and *Bcl6* all of which are up regulated in young adult and older adult satellite cells compared to satellite cells isolated from adolescent mice. Interestingly, further analysis of recent transcriptional data comparing young adult to geriatric satellite cells[17] shows a significant increase in the expression of JAK/STAT signaling.

Aged skeletal myofibers secrete heightened levels of bFGF that impede quiescence and ultimately affect the functional capacity of resident satellite cells[36]. It is also plausible that extrinsic activators such as bFGF, interleukins, PDGF or EGF present in adult skeletal

muscle may also act on satellite cells to alter their intrinsic functional capacity via activation of JAK/STAT signaling. Chronic inflammation is a common characteristic of diseased (dystrophic) and/or aged skeletal muscle. Increased infiltration of inflammatory cells in combination with circulating pro-inflammatory cytokines (Interleukins, TNFα) have a detrimental effect on tissue regenerative potential[37]. The JAK/STAT signaling pathway plays a critical role in transduction of extracellular signals from cytokines and growth factors involved in proliferation, migration, apoptosis, survival and oncogenesis[38]. Therefore, another possible cause of increasing JAK/STAT signaling in adulthood is the increasing levels of inflammatory cells in ageing muscle tissue.

Our data suggests that activation of JAK/STAT signaling in satellite cells profoundly inhibits their capacity to undergo symmetric stem cell expansion. Previous studies from our lab have indicated that the regulation of the level of symmetric stem cell division by Wnt7a/Fzd7 signaling is a central mechanism regulating satellite cell homeostasis and that enhancing symmetric stem cell division markedly augments muscle repair[39–41]. The Par polarity complex, consisting of Par3, Par6, and aPKC plays a central role in integrating Wnt and Notch signaling into the regulation of asymmetric stem cell divisions[42]. Interestingly, MAPK and p38 kinases are activated in satellite cells in a Par-complex dependant manner[12,18,19,27]. Furthermore, the Par-complex is implicated in the activation of aPKC and Stat3 in breast cancer stem cells[43]. These findings suggest that Jak2/Stat3 signaling plays a role in the function of the Par polarity complex.

Our experiments provide strong support for the hypothesis that with increasing age activation of JAK/STAT signaling in satellite cells significantly contributes to myogenic commitment and results in their regenerative deficiency. Our data supports recent reports indicating that aged satellite cells exhibit enhance myogenic commitment[18,19,36]. We found that treatment with small molecule inhibitors of JAK/STAT signaling resulted in increased numbers of satellite cells, enhanced muscle repair and enhanced functional performance. While intramuscular injection of JAK/STAT inhibiters may also be acting on other cells in the tissue milieu, our experiments nevertheless indicate that the enhancement of muscle repair can be stimulated using small drugs that have been identified on the basis of their ability to modulate the function of satellite cells.

Therefore, we conclude that aberrant JAK/STAT signaling is an important contributor to satellite cell dysfunction in adulthood. Together these results reveal intrinsic differences that distinguish young and adult satellite cells and suggest a promising therapeutic approach for the stimulation of muscle regeneration.

ONLINE METHODS

Animal experiments

For this study we used the following mouse lines bred in our animal facility: *Pax7-ZsGreen mice*[44], *mdx* mice (*C57BL/10ScSn-Dmdmdx/J* - Jackson Laboratories, Harbour Maine - #001801), and *SV129* mice (Charles River laboratories, St. Constant QC). All mice were housed under standard conditions and allowed free access to food and water *ad libitum*. All

experiments were performed in accordance with University of Ottawa guidelines for animal handling and animal care determined by the University of Ottawa Animal Care Committee.

Immunohistochemistry and FACS isolation

Immunohistochemistry was performed as described earlier[45,46] using the following antibodies: Pax7, MyHC (MF20), Dystrophin (7A10) from the (DSHB), α7 integrin (UBC Ablab), β1 integrin, Pdgfrα, and CD34 (eBioscience), CXCR4 (BD Bioscience), Mcadherin (Millipore), Laminin (Sigma), ZsGreen (Clontech), devMyHC (Leica), MyoD (C-20 Santa Cruz) along with appropriate secondary antibodies (Molecular Probes, BD Bioscience) Skeletal muscles from heterozygous Pax7-ZsGreen mice were isolated at defined stages: 3 weeks (Adolescent - hind limb), 2–4 months (Young Adult - hind limb) and 18 ± 2 months (Older adult – hind limb). Muscles were aseptically dissected, minced and digested in a dispase/collagenase solution (1 mg/ml collagenase, 4 mg/ml Dispase II, Roche) for 25 minutes at 37°C. The digested muscle slurry was briefly triturated after 15 min of incubation and returned to the incubator. The slurry was subsequently diluted with PBS containing 10% fetal bovine serum and 2 mM EDTA (FACS sorting medium), filtered through 70 μm Netwell cell strainers (Costar), and pelleted at 1700 rpm for 5 min (Thermo IEC Centra CL2). Cell pellets were gently resuspended in FACS buffer and incubated/agitated with primary antibodies and when appropriate secondary antibodies for 9 min on ice. Cells were subsequently washed in FACS buffer, pelleted and filtered through 30 μM filters (Miltenyi Biotech) prior to FACS sorting. Cells were separated on a MoFlo cytometer (DakoCytomation) equipped with 3 lasers. Sorting gates were strictly defined based on age of sample or in the case of a negative control for *Pax7-ZsGreen*, wild type *SV129* mice. We routinely stain FACS sorted cells in these experiments and ~99% of the cells express Pax7.

NanoPro immunoassay

ZsGreen-expressing satellite cells were isolated by FACS from adolescent, young adult and older adult mice, and pelleted by centrifugation at 8000 rpm for 5 min at 4°C. Cell lysis was performed with Bicine/CHAPS lysis buffer (20mM Bicine, pH 7.5, 0.6% CHAPS) supplemented with 1X DMSO and Aqueous Inhibitor Mixes (ProteinSimple). Cells were lysed for 30 min on ice and lysates were cleared by centrifugation at 14,800 rpm for 15 min at 4°C. Analysis of satellite cell lysates by capillary isoelectric focusing using the NanoPro™ 1000 were performed according to manufacturer's protocol. Immunoprobing was performed using phospho-Stat3 Tyr705 (Cell Signaling) and Hsp70 (Abcam) antibodies. Chemiluminescent signals were analyzed and quantified with Compass software (ProteinSimple).

Myofiber culture, satellite cell transplantation and muscle injury

Myofiber culture and transplantation of freshly sorted satellite cells was performed as described earlier[47,48]. Enumeration of satellite cells was conducted on at least 15 fibers per replicate at 72 h. These experiments were conducted in at least biological triplicate from each condition at each age time point (e.g. over 45 myofibers in total/condition). Furthermore, at 0 h due to the fewer number of satellite cells per myofiber we counted 30 fibers per condition in biological triplicate (90 fibers in total). Myofiber feret size was

measured as described previously[49]. Treatment of satellite cells with siRNAs: siStat3 (Catalogue # L-040794-01-0005 Dhramacon) siJak2 (Catalogue # L-040118-00-0005 Dharmacon). siRNA transfection was conducted using RNAiMAX (Life Technologies) on freshly sorted satellite cells on ice for 3 h or on single myofibres as described earlier5. Treatment of satellite cells with inhibitors: (50μM) 5,15-diphenylporphrine (5,15-DPP Sigma Aldrich), (5 μM) Tyrphostin AG 490 (Tyr AG 490 Sigma Aldrich) was performed on ice for 3 h or on single fibres as described earlier5. TA muscles of young adult mice were injured with 50 μl of cardiotoxin (10μM). Direct injection (25 μl) of 5,15 DPP (100μM) and Tyr AG 490 (10μM) was conducted into regenerating TA muscles 48 h following cardiotoxin treatment. For functional measurements, EDL muscles from young adult (3 months of age) were injured with CTX at day 0, injected IM with small molecules at day 3 and sacrificed at day 10. Muscles were carefully dissected, attached to an electrode with a force sensor (305B-LR, Aurora Scientific, Inc., Aurora, ON, Canada), and incubated at 25°C in buffered physiological saline (Krebs-Ringer) supplemented with glucose and carbogen. Maximal force was generated by a 25V electrical stimulation at a frequency of 100 Hz for 500 ms. Muscle fatigue was assessed by stimulating muscles at 50 Hz for 200 ms every second until muscles reached 50% of their initial force. Thereafter, muscle length and weight were measured and specific muscle force was calculated ((maximal force x optimal fiber length x muscle density) / muscle mass).

Microarray and bioinformatic analysis

FACS Purified ZsGreen-expressing cells were obtained from pooled populations of adolescent (n=6), young adult (n=8) and older adult (n=8) muscles. Total RNA was extracted from each replicate using the Picopure RNA isolation kit (Applied Biosystems) and concentrated using the RNA Clean and Concentrator-5 kit (Zymo Research) according to the manufacturer's instructions. qPCR analysis was conducted as described earlier3 with the following primer sequences 5' to 3': JunD ex 1 F ATCTTGGGCTGCTCAAACTC, JunD ex1 R AACTGCTCAGGTTGGCGTAG, Bcl2 ex1 F GAGCGTCAACAGGGAGATGT, Bcl2 ex2 R CTCACTTGTGGCCCAGGTAT, Bcl6 ex4 F CCTGAGGGAAGGCAATATCA, Bcl6 ex5 R CGGCTGTTCAGGAACTCTTC, Cebpd ex1 F CGCAGACAGTGGTGAGCTT, Cebpd ex1 R CTTCTGCTGCATCTCCTGGT, Fos ex1 F ATGGGCTCTCCTGTCAACAC, Fos ex2 R GACACGGTCTTCACCATTCC, Myc ex2 F TCCTGTACCTCGTCCGATTC, Myc ex3 R GGTTTGCCTCTTCTCCACAG, Egfr ex1 F ACACTGCTGGTGTTGCTGAC, Egfr ex2 R CCCAAGGACCACTTCACAGT, Ar ex4 F CGGACATGACAACAACCAAC, Ar ex5 R ATCTGGTCATCCACATGCAA, gp130 ex2 F GGAGCAGGTCACTGTCATCA, gp130 ex3 R CTTCCCCTCATTCACAATGC, Pim1 ex4 F CGACATCAAGGACGAGAACA, Pim1 ex5 R TCCGCAGACCATGTCATAGA, Socs3 ex2 F GCAAGCTGCAGGAGAGCGGATT, Socs3 ex2 R AAGAAGTGGCGCTGGTCCGA. Sample RNA quality was assessed on the Agilent Bioanalyzer 2100 using the RNA 6000 nano chip (Agilent Technologies, Santa Clara). Microarray target preparation was achieved using the WT Expression kit (Ambion) and the Genechip terminal labelling kit (Affymetrix). The microarray data was collected using Genechip mouse gene 1.0 ST arrays (Affymetrix). R-2.10.0 with the XPS library was used to import CEL files, RMA normalize and perform DABG (detection above background) calls. Anti-genomic background and the metacore exon level definition were

used. The RMA expression values are log2 transformed. Probe annotation was extracted from ensembl v62 using the biomart R package and used to map transcript cluster ids to genes. The resulting five Mogene v1.0ST microarray data sets are referred to as adolescent, young adult and older adult for subsequent methods of analysis. Genes that met the criteria of a log-fold change of greater than one (that is, 2-fold cut-off) were used for further analysis by DAVID (http://david.abcc.ncifcrf.gov/home.jsp)[50,51] or Gene set enrichment analysis (GSEA)[52]. The NES score corresponds to a weighted Kolmogorov-Smirnov statistic and reflects the degree to which a signaling pathway is over represented at the extremities of the ranked list[53]. All microarray data have been deposited in GEO and are available in the series GSE47401.

Statistical analysis

A minimum of three replicates were analysed for each experiment presented. Data are presented as standard error of the mean (Microsoft Excel), Statistical analysis was conducted using the Student's t-test method of determining inference based on small samples. *Indicates a $p < 0.05$ while ** indicates a $p < 0.01$ and *** indicates a $p < 0.001$.

Supplementary Material

Refer to Web version on PubMed Central for supplementary material.

ACKNOWLEDGEMENTS

We thank Paul Oleynik for conducting cell sorting and providing guidance regarding FACS isolation and analysis. We thank Jennifer Ritchie for mouse husbandry, Alexander Grayston for his help with myofibers counts, and Gareth Palidwor for RMA normalization of microarray data sets and constructive discussions. We thank Dr. Vahab Soleimani for constructive discussions and access to unpublished microarray data. We thank M. Kyba, University of Minnesota, for the *Pax7-ZsGreen* mice. F. Price was supported by the Canadian Stem Cell Network and a Doctoral Research Award from the Canadian Institutes of Health Research. J. von Maltzahn was supported by a grant from the German Research Foundation (MA-3975/2-1). C.F. Bentzinger was supported by the Swiss National Science Foundation. M. Rudnicki holds the Canada Research Chair in Molecular Genetics. These studies were carried out with support of grants to M. Rudnicki. from the US National Institutes for Health (R01AR044031), the Canadian Institutes for Health Research (MOP-81288), the Stem Cell Network, and the Ontario Ministry of Economic Development and Innovation.

REFERENCES

1. Mauro A. Satellite cell of skeletal muscle fibers. J Biophys Biochem Cytol. 1961; 9:493–495. [PubMed: 13768451]
2. Schultz E, Gibson MC, Champion T. Satellite cells are mitotically quiescent in mature mouse muscle: an EM and radioautographic study. J Exp Zool. 1978; 206:451–456. [PubMed: 712350]
3. Montarras D, et al. Direct isolation of satellite cells for skeletal muscle regeneration. Science. 2005; 309:2064–2067. [PubMed: 16141372]
4. Collins CA, et al. Stem cell function, self-renewal, and behavioral heterogeneity of cells from the adult muscle satellite cell niche. Cell. 2005; 122:289–301. [PubMed: 16051152]
5. Kuang S, Kuroda K, Le Grand F, Rudnicki MA. Asymmetric self-renewal and commitment of satellite stem cells in muscle. Cell. 2007; 129:999–1010. [PubMed: 17540178]
6. Zammit PS, et al. Muscle satellite cells adopt divergent fates: a mechanism for self-renewal? J Cell Biol. 2004; 166:347–357. [PubMed: 15277541]
7. Carlson ME, Conboy IM. Loss of stem cell regenerative capacity within aged niches. Aging Cell. 2007; 6:371–382. [PubMed: 17381551]

8. Augustin H, Partridge L. Invertebrate models of age-related muscle degeneration. Biochim Biophys Acta. 2009; 1790:1084–1094. [PubMed: 19563864]
9. Grounds MD. Age-associated changes in the response of skeletal muscle cells to exercise and regeneration. Ann N Y Acad Sci. 1998; 854:78–91. [PubMed: 9928422]
10. Allbrook DB, Han MF, Hellmuth AE. Population of muscle satellite cells in relation to age and mitotic activity. Pathology. 1971; 3:223–243. [PubMed: 4107201]
11. Shefer G, Van de Mark DP, Richardson JB, Yablonka-Reuveni Z. Satellite-cell pool size does matter: defining the myogenic potency of aging skeletal muscle. Dev Biol. 2006; 294:50–66. [PubMed: 16554047]
12. Conboy IM, Rando TA. The regulation of Notch signaling controls satellite cell activation and cell fate determination in postnatal myogenesis. Dev Cell. 2002; 3:397–409. [PubMed: 12361602]
13. Carlson ME, Hsu M, Conboy IM. Imbalance between pSmad3 and Notch induces CDK inhibitors in old muscle stem cells. Nature. 2008; 454:528–532. [PubMed: 18552838]
14. Conboy IM, Conboy MJ, Smythe GM, Rando TA. Notch-mediated restoration of regenerative potential to aged muscle. Science. 2003; 302:1575–1577. [PubMed: 14645852]
15. Brack AS, et al. Increased Wnt signaling during aging alters muscle stem cell fate and increases fibrosis. Science. 2007; 317:807–810. [PubMed: 17690295]
16. Brack AS, Rando TA. Intrinsic changes and extrinsic influences of myogenic stem cell function during aging. Stem Cell Rev. 2007; 3:226–237. [PubMed: 17917136]
17. Sousa-Victor P, et al. Geriatric muscle stem cells switch reversible quiescence into senescence. Nature. 2014; 506:316–321. [PubMed: 24522534]
18. Cosgrove BD, et al. Rejuvenation of the muscle stem cell population restores strength to injured aged muscles. Nat Med. 2014
19. Bernet JD, et al. p38 MAPK signaling underlies a cell-autonomous loss of stem cell self-renewal in skeletal muscle of aged mice. Nat Med. 2014; 20:265–271. [PubMed: 24531379]
20. Bentzinger CF, Rudnicki MA. Rejuvenating aged muscle stem cells. Nat Med. 2014; 20:234–235. [PubMed: 24603790]
21. Yablonka-Reuveni Z, Seger R, Rivera AJ. Fibroblast growth factor promotes recruitment of skeletal muscle satellite cells in young and old rats. J Histochem Cytochem. 1999; 47:23–42. [PubMed: 9857210]
22. Neal A, Boldrin L, Morgan JE. The satellite cell in male and female, developing and adult mouse muscle: distinct stem cells for growth and regeneration. PLoS One. 2012; 7:e37950. [PubMed: 22662253]
23. Bosnakovski D, et al. Prospective isolation of skeletal muscle stem cells with a Pax7 reporter. Stem Cells. 2008; 26:3194–3204. [PubMed: 18802040]
24. Subramanian A, et al. Gene set enrichment analysis: a knowledge-based approach for interpreting genome-wide expression profiles. Proc Natl Acad Sci U S A. 2005; 102:15545–15550. [PubMed: 16199517]
25. Conboy IM, et al. Rejuvenation of aged progenitor cells by exposure to a young systemic environment. Nature. 2005; 433:760–764. [PubMed: 15716955]
26. Toth KG, et al. IL-6 induced STAT3 signalling is associated with the proliferation of human muscle satellite cells following acute muscle damage. PLoS One. 2011; 6:e17392. [PubMed: 21408055]
27. Troy A, et al. Coordination of satellite cell activation and self-renewal by Par-complex-dependent asymmetric activation of p38alpha/beta MAPK. Cell Stem Cell. 2012; 11:541–553. [PubMed: 23040480]
28. Eriksen KW, et al. Constitutive STAT3-activation in Sezary syndrome: tyrphostin AG490 inhibits STAT3-activation, interleukin-2 receptor expression and growth of leukemic Sezary cells. Leukemia. 2001; 15:787–793. [PubMed: 11368440]
29. Uehara Y, Mochizuki M, Matsuno K, Haino T, Asai A. Novel high-throughput screening system for identifying STAT3-SH2 antagonists. Biochem Biophys Res Commun. 2009; 380:627–631. [PubMed: 19285012]

30. Pasut A, Jones AE, Rudnicki MA. Isolation and Culture of Individual Myofibers and their Satellite Cells from Adult Skeletal Muscle. Journal of visualized experiments : JoVE. 2013
31. Launay T, Noirez P, Butler-Browne G, Agbulut O. Expression of slow myosin heavy chain during muscle regeneration is not always dependent on muscle innervation and calcineurin phosphatase activity. Am J Physiol Regul Integr Comp Physiol. 2006; 290:R1508–R1514. [PubMed: 16424085]
32. Shuai K, Liu B. Regulation of JAK-STAT signalling in the immune system. Nat Rev Immunol. 2003; 3:900–911. [PubMed: 14668806]
33. Megeney LA, Perry RL, LeCouter JE, Rudnicki MA. bFGF and LIF signaling activates STAT3 in proliferating myoblasts. Dev Genet. 1996; 19:139–145. [PubMed: 8900046]
34. Yang Y, et al. STAT3 induces muscle stem cell differentiation by interaction with myoD. Cytokine. 2009; 46:137–141. [PubMed: 19223199]
35. McKay BR, et al. Elevated SOCS3 and altered IL-6 signaling is associated with age-related human muscle stem cell dysfunction. Am J Physiol Cell Physiol. 2013; 304:C717–C728. [PubMed: 23392112]
36. Chakkalakal JV, Jones KM, Basson MA, Brack AS. The aged niche disrupts muscle stem cell quiescence. Nature. 2012; 490:355–360. [PubMed: 23023126]
37. Jang YC, Sinha M, Cerletti M, Dall'Osso C, Wagers AJ. Skeletal muscle stem cells: effects of aging and metabolism on muscle regenerative function. Cold Spring Harb Symp Quant Biol. 2011; 76:101–111. [PubMed: 21960527]
38. Harrison DA. The Jak/STAT pathway. Cold Spring Harb Perspect Biol. 2012; 4
39. Le Grand F, Jones AE, Seale V, Scime A, Rudnicki MA. Wnt7a activates the planar cell polarity pathway to drive the symmetric expansion of satellite stem cells. Cell Stem Cell. 2009; 4:535–547. [PubMed: 19497282]
40. von Maltzahn J, Bentzinger CF, Rudnicki MA. Wnt7a-Fzd7 signalling directly activates the Akt/mTOR anabolic growth pathway in skeletal muscle. Nat Cell Biol. 2012; 14:186–191. [PubMed: 22179044]
41. Bentzinger CF, et al. Fibronectin regulates Wnt7a signaling and satellite cell expansion. Cell Stem Cell. 2013; 12:75–87. [PubMed: 23290138]
42. Tepass U. The apical polarity protein network in Drosophila epithelial cells: regulation of polarity, junctions, morphogenesis, cell growth, and survival. Annu Rev Cell Dev Biol. 2012; 28:655–685. [PubMed: 22881460]
43. McCaffrey LM, Montalbano J, Mihai C, Macara IG. Loss of the Par3 polarity protein promotes breast tumorigenesis and metastasis. Cancer Cell. 2012; 22:601–614. [PubMed: 23153534]
44. Bosnakovski D, et al. Prospective isolation of skeletal muscle stem cells with a Pax7 reporter. Stem Cells. 2008; 26:3194–3204. [PubMed: 18802040]
45. von Maltzahn J, Bentzinger CF, Rudnicki MA. Wnt7a-Fzd7 signaling directly activates the Akt/mTOR anabolic growth pathway in skeletal muscle. Nat Cell Biol. 2012; 14:186–191. [PubMed: 22179044]
46. Price FD, et al. Canonical Wnt signaling induces a primitive endoderm metastable state in mouse embryonic stem cells. Stem Cells. 2013; 31:752–64. [PubMed: 23307624]
47. Pasut A, Jones AE, Rudnicki MA. Isolation and Culture of Individual Myofibers and their Satellite Cells from Adult Skeletal Muscle. J Vis Exp. 2013; (73):e50074. [PubMed: 23542587]
48. Bentzinger CF, et al. Fibronectin regulates Wnt7a signaling and satellite cell expansion. Cell Stem Cell. 2013; 12:75–87. [PubMed: 23290138]
49. Briguet A, Courdier-Fruh I, Foster M, Meier T, Magyar JP. Histological parameters for the quantitative assessment of muscular dystrophy in the mdx-mouse. Neuromuscul Disord. 2004; 14:675–682. [PubMed: 15351425]
50. Huang da W, Sherman BT, Lempicki RA. Bioinformatics enrichment tools: paths toward the comprehensive functional analysis of large gene lists. Nucleic Acids Res. 2009; 37:1–13. [PubMed: 19033363]
51. Huang da W, Sherman BT, Lempicki RA. Systematic and integrative analysis of large gene lists using DAVID bioinformatics resources. Nat Protoc. 2009; 4:44–57. [PubMed: 19131956]

52. Mootha VK, et al. PGC-1alpha-responsive genes involved in oxidative phosphorylation are coordinately downregulated in human diabetes. Nat Genet. 2003; 34:267–273. [PubMed: 12808457]

53. Subramanian A, et al. Gene set enrichment analysis: a knowledge-based approach for interpreting genome-wide expression profiles. Proc Natl Acad Sci U S A. 2005; 102:15545–15550. [PubMed: 16199517]

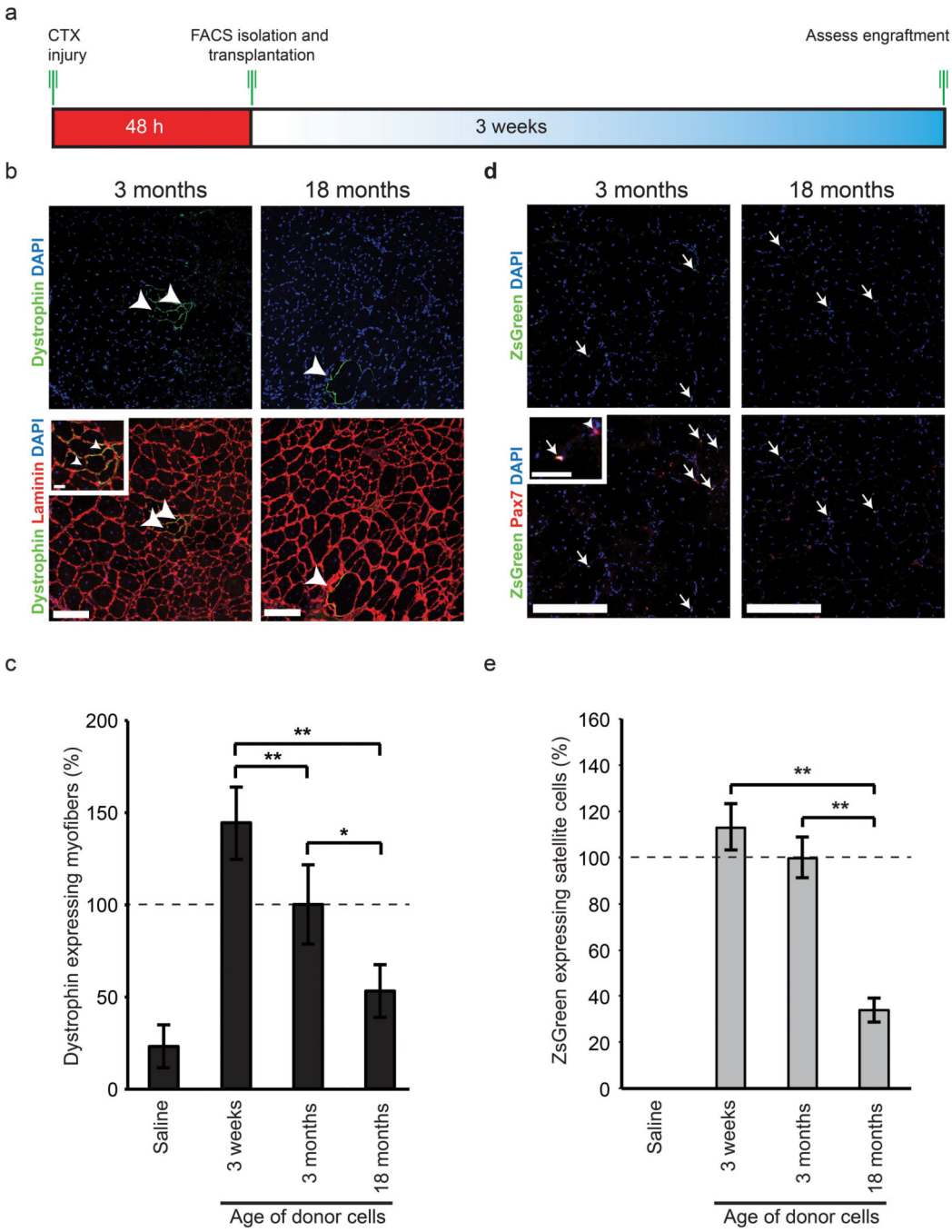

Figure 1.

Increasing age negatively affects the engraftment capacity of satellite cells. (**a**) Experimental schematic outlining the FACS isolation and immediate transplantation into regenerating TA muscle of immunosuppressed *mdx* mice between the ages of 6 to 8 weeks. (**b**) The intrinsic contribution of satellite cells to muscle regeneration in 2–4 month *mdx* mice (n=9 for each time point) with respect to increasing age. Dystrophin (green), laminin (red) and DAPI (blue) staining in *mdx* TA muscle 3 weeks following transplantation. Arrowheads designate dystrophin positive fibers. Adolescent data is found in Supplementary Fig. 2. Scale bars

denote 100μm and 20μm (inset) (**c**) Quantification of the percentage of dystrophin positive fibers post transplantation of age related satellite cell populations. Values are relative to 3-month-old satellite cell transplants. * $p < 0.05$, ** $p < 0.01$. (**d**) Intrinsic repopulating capacity of transplanted cells into the satellite cell niche. Immunofluorescence of Pax7 (red) and ZsGreen (green) 3 weeks post transplantation of age specific satellite cells into cardiotoxin injured TA muscle of *mdx* mice. Arrows designate satellite cells both positive for ZsGreen and Pax7 while arrowheads designate host $Pax7^+$ satellite cells. Scale bar denotes 100μm and 20μm (inset). High magnification images of Pax7 and ZsGreen along with adolescent images are found in Supplemental Fig. 2. (**e**) Quantification of the repopulating capacity associated with transplanted satellite cells from young adult and older adult muscle as evidenced by enumeration of double positive $Pax7^+/ZsGreen^+$ cells in relation to total $Pax7^+$ satellite cells. * $p < 0.05$, ** $p < 0.01$.

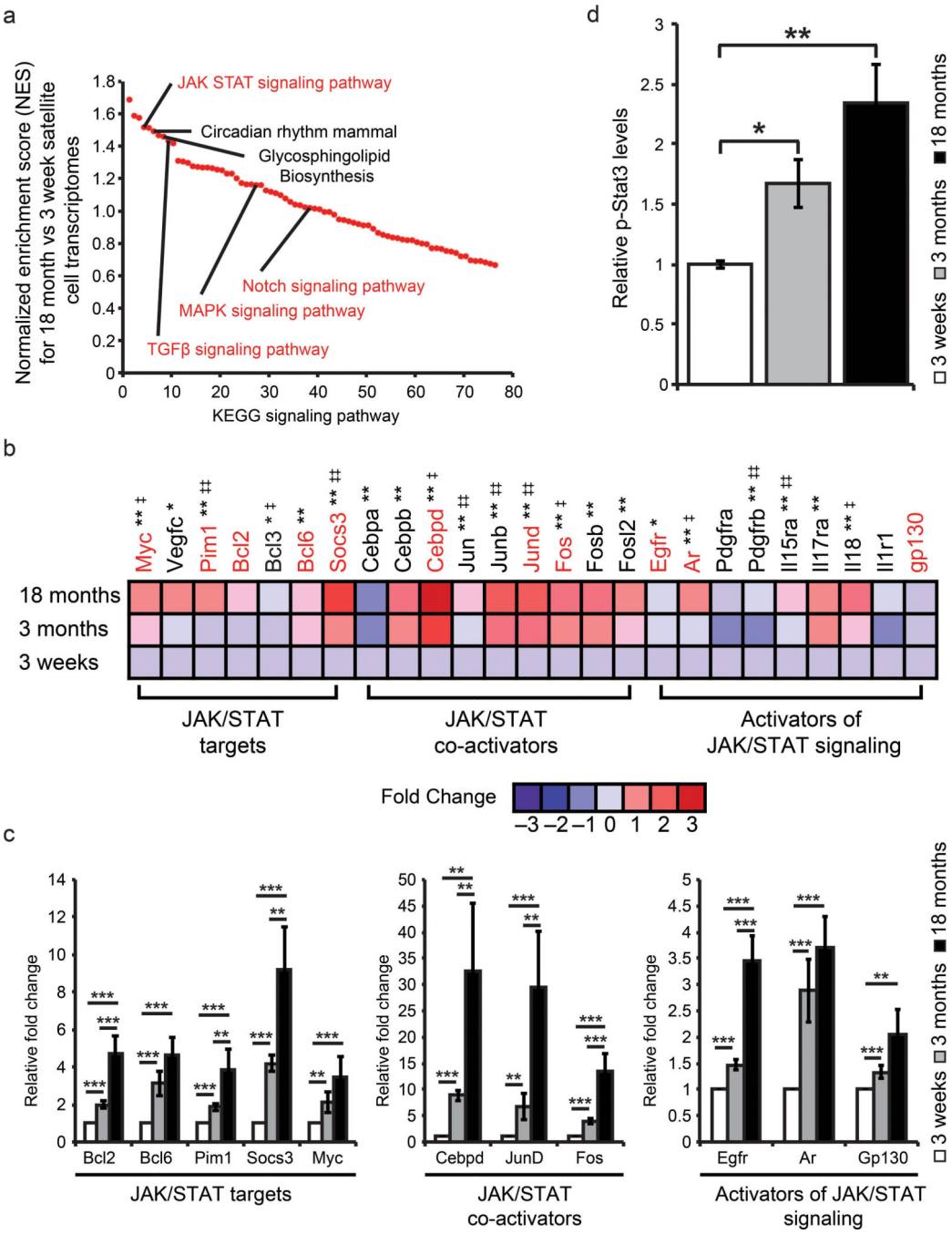

Figure 2.

The transcriptional profile of adult satellite cells is enriched for JAK/STAT signaling pathway members and interactors. (**a**) Comparison between genes enriched (>2 fold) in adolescent versus older adult satellite cells based on KEGG signaling pathway enrichment. Signaling pathways are ranked based on their normalized enrichment score (NES). Signaling pathways connected with skeletal muscle regeneration are highlighted in red. **(b)** Fold changes based on Log2 transformed RMA values from adolescent, young adult and older adult satellite cells were used to generate global ratio heat maps. Red indicates genes that

increase in expression while blue represents a decrease. * Designates significance between adolescent and young adult where * $p < 0.05$, ** $p < 0.01$. ‡ Designates significance between young adult and older adult where ‡ $p < 0.05$ ‡‡ $p < 0.01$. Genes highlighted in red are validated by QPCR in panel c. Data represents pooled replicates of adolescent ($n=5$), young adult (n=8), older adult (n=8) conducted in biological triplicate. (**c**) QPCR validation of microarray data supports transcriptional changes observed between adolescent, young adult and older adult satellite cells. Data are presented as the mean ± SEM of 3 biological replicates of freshly sorted satellite cells normalized to GAPDH. (**d**) Quantification of p-Stat3 protein expression from age-related satellite cell samples (Supplementary Fig. 3f) normalized to Hsp70 protein expression to account for loading. Data represent the mean ± STD of 3 biological replicates ($n=3$). * $p < 0.05$, ** $p < 0.01$.

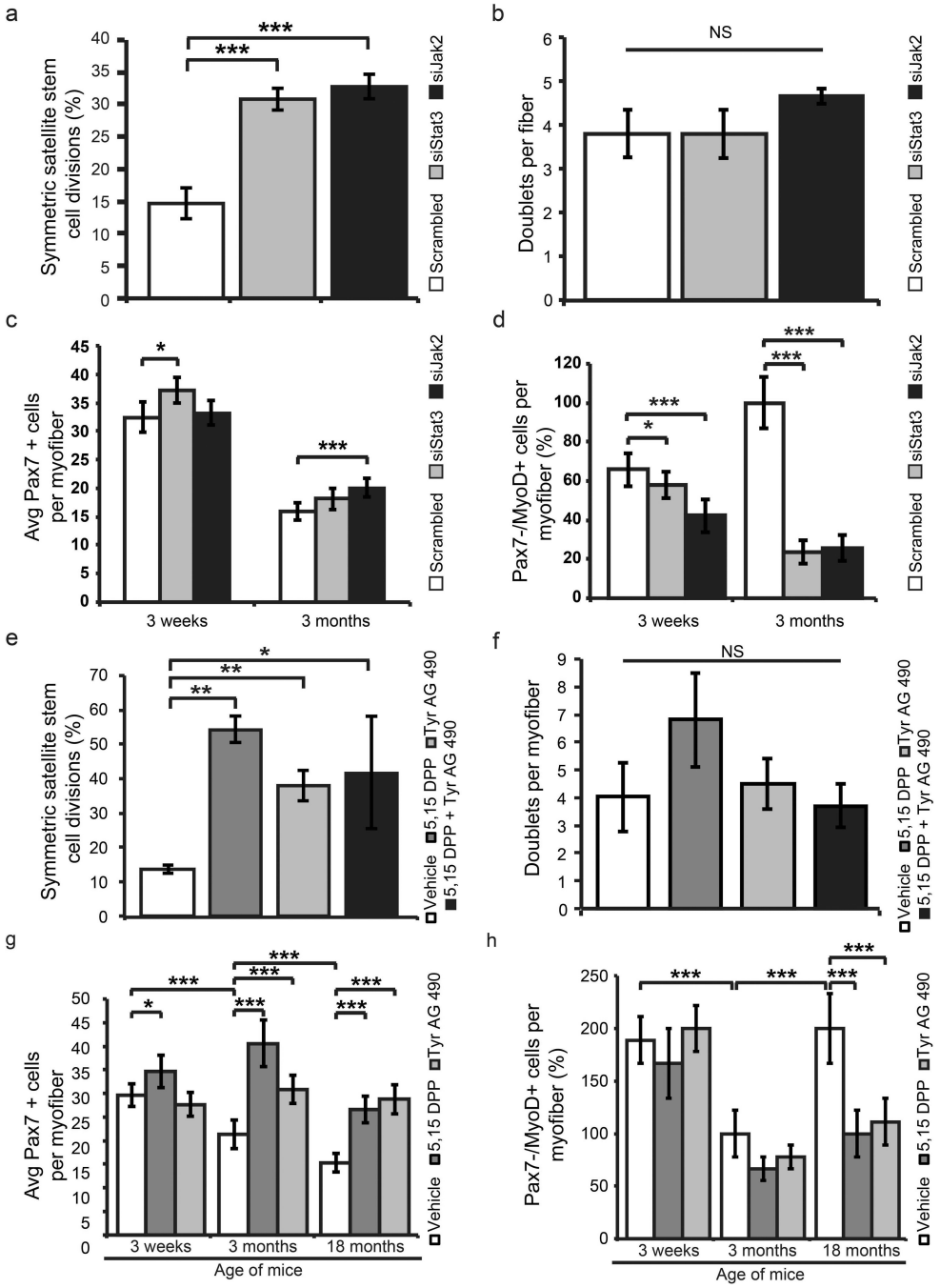

Figure 3.

Inhibition of JAK/STAT signaling rescues the proliferation defect of satellite cells from older adult muscle. (**a**) Effect of siRNA knockdown of Jak2 or Stat3 on the symmetric divisions of satellite stem cells ($Pax7^{+}/Myf5^{-}$) on myofibers from *$Myf5^{Cre}$; R26R-YFP* cultured for 42h *in vitro*. (**b**) Quantification of the total number of dividing satellite cells on single fibers cultured for 42 h *in vitro* following siRNA knockdown of Jak2 or Stat3. (**c**) Quantification of the average number of $Pax7^{+}$ satellite cells per fiber for each age stage following siRNA knockdown. (**d**) Quantification of the percentage of committed satellite

cells ($Pax7^{-}/MyoD^{+}$) present on single myofibers following 72 h culture following treatment with siRNAs against Stat3 or Jak2. (**e**) Quantification of symmetric satellite stem cell divisions following JAK/STAT inhibitor treatment for 42 h on myofibers from young adult mice. (**f**) Quantification of the total number of dividing satellite cells on single fibers cultured for 42 h *in vitro* following pharmacological inhibition of Jak2 or Stat3. (**g**) Quantification of the average number of $Pax7^{+}$ satellite cells per fiber for each age stage following treatment with small molecules. (**h**) Quantification of the percentage of committed satellite cells ($Pax7^{-}/MyoD^{+}$) present on single fibers following 72 h culture in the presence of JAK/STAT inhibitors. Data represent the mean ± SEM conducted in at least biological triplicate. * $p < 0.05$, ** $p < 0.01$, *** $p < 0.001$.

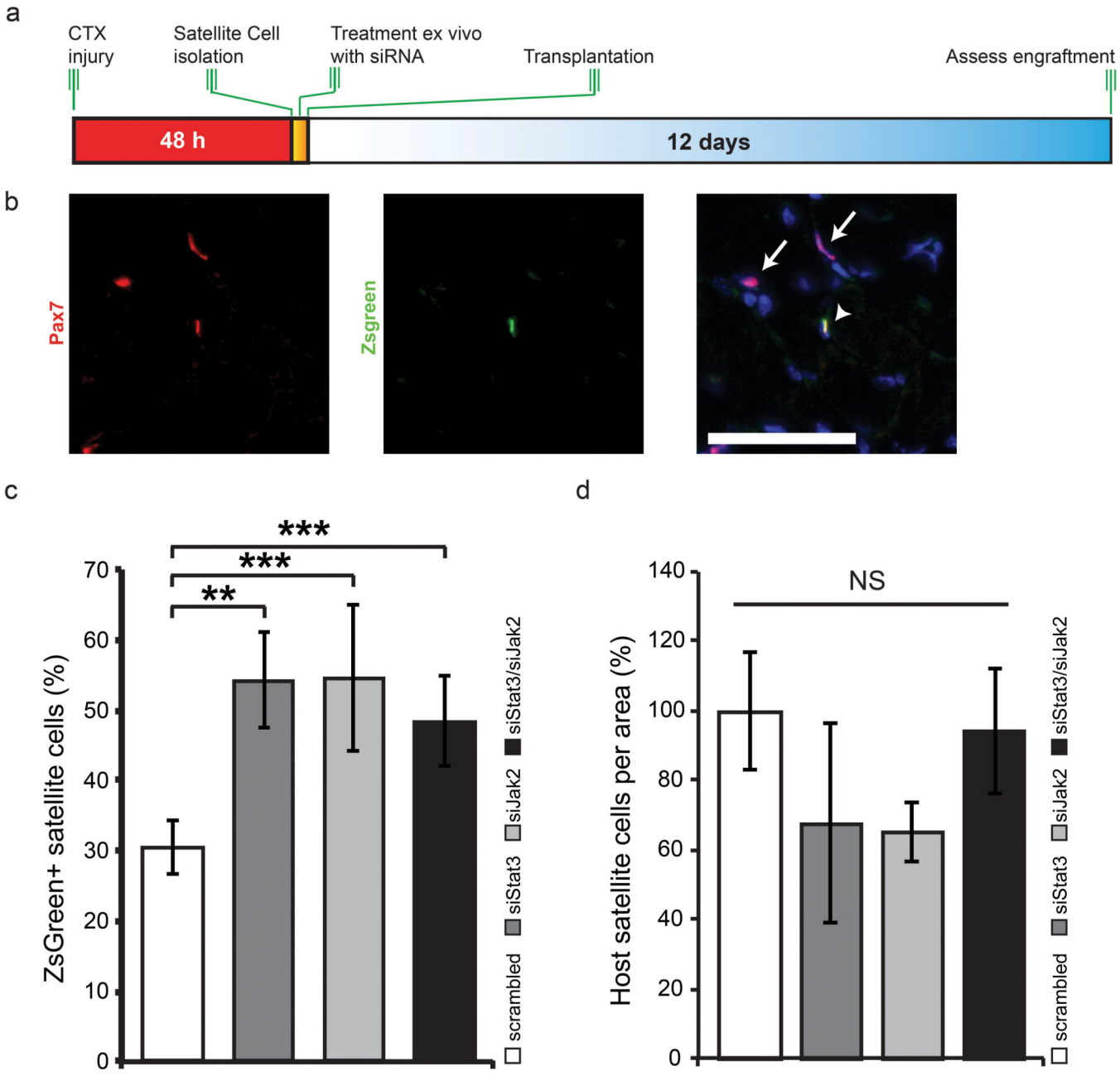

Figure 4.

Knockdown of JAK/STAT pathway members ameliorates the engraftment potential of adult satellite cells. (**a**) Experimental schematic outlining the FACS isolation, treatment *ex vivo* with siScrambled, siStat3, siJak2 or a combination of siStat3 and siJak2 followed by transplantation into CTX treated TA muscle of C57Bl/6 mice. (**b**) Representative images from *ex vivo* siRNA treated satellite cells. Pax7 (green), ZsGreen (red) and DAPI (blue) staining in C57Bl/6 TA muscle 12 d following transplantation. Arrows designate host satellite cells while arrowheads designate a donor-derived satellite cell. Scale bar denotes 50 μm. (**c**) Quantification of the percentage of ZsGreen^{+} satellite cells following siRNA

knockdown and transplantation. (**d**) Quantification of the host satellite cells per area following siRNA knockdown and transplantation.

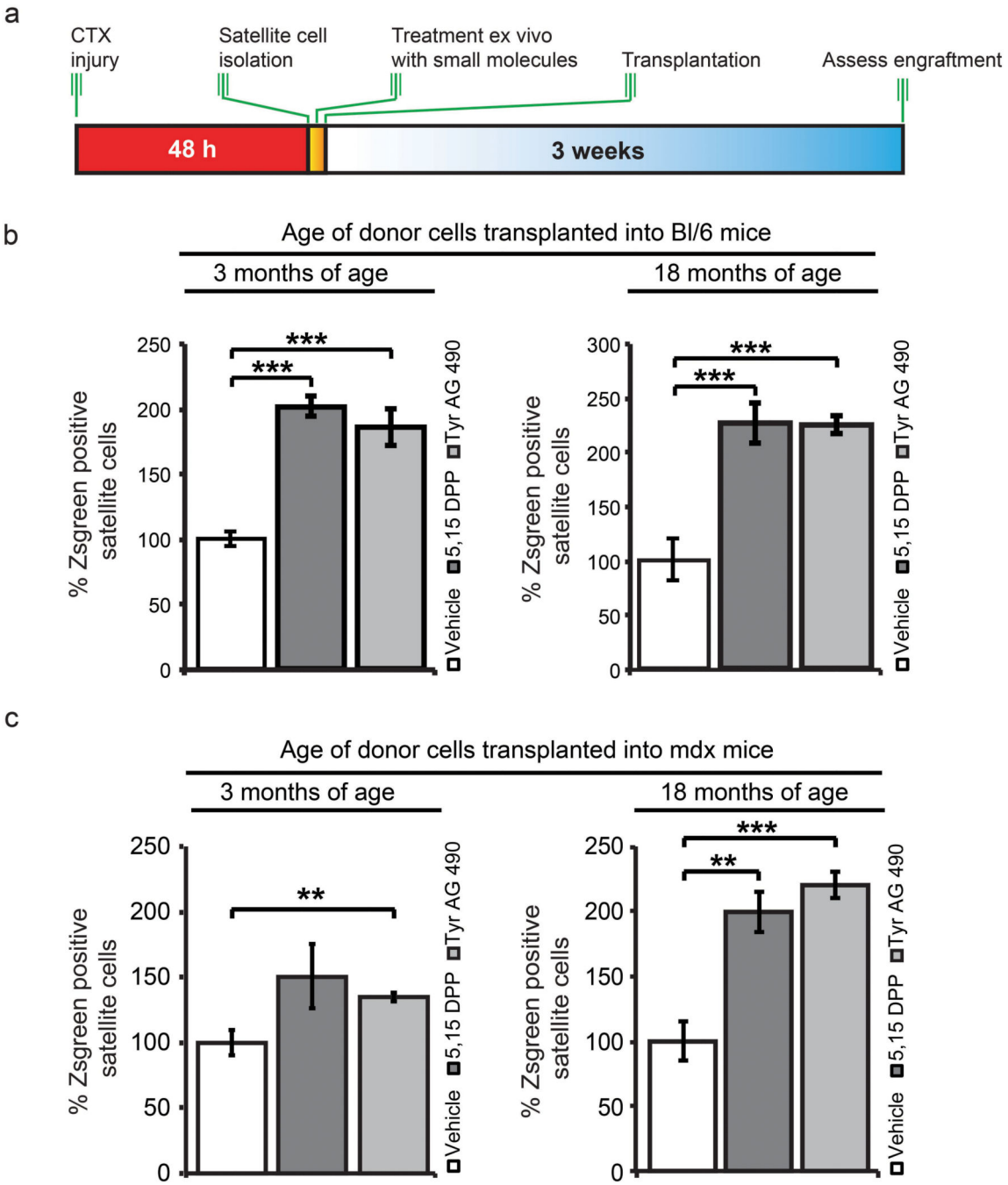

Figure 5.

Administration of small molecule JAK/STAT inhibitors *ex vivo* prior to transplantation into young adult mice enhances engraftment. (**a**) Schematic for *ex vivo* treatment of freshly sorted satellite cells with JAK/STAT inhibitors prior to transplantation. (**b**) Quantification of young adult and older adult donor satellite cells following *ex vivo* treatment with JAK/STAT inhibitors transplanted into C57Bl/6 mice. (**c**) Quantification of young adult and older adult donor satellite cells following *ex vivo* treatment with JAK/STAT inhibitors transplanted into

mdx mice. Data represent the mean ± SEM conducted in biological triplicate. ** $p < 0.01$, *** $p < 0.001$

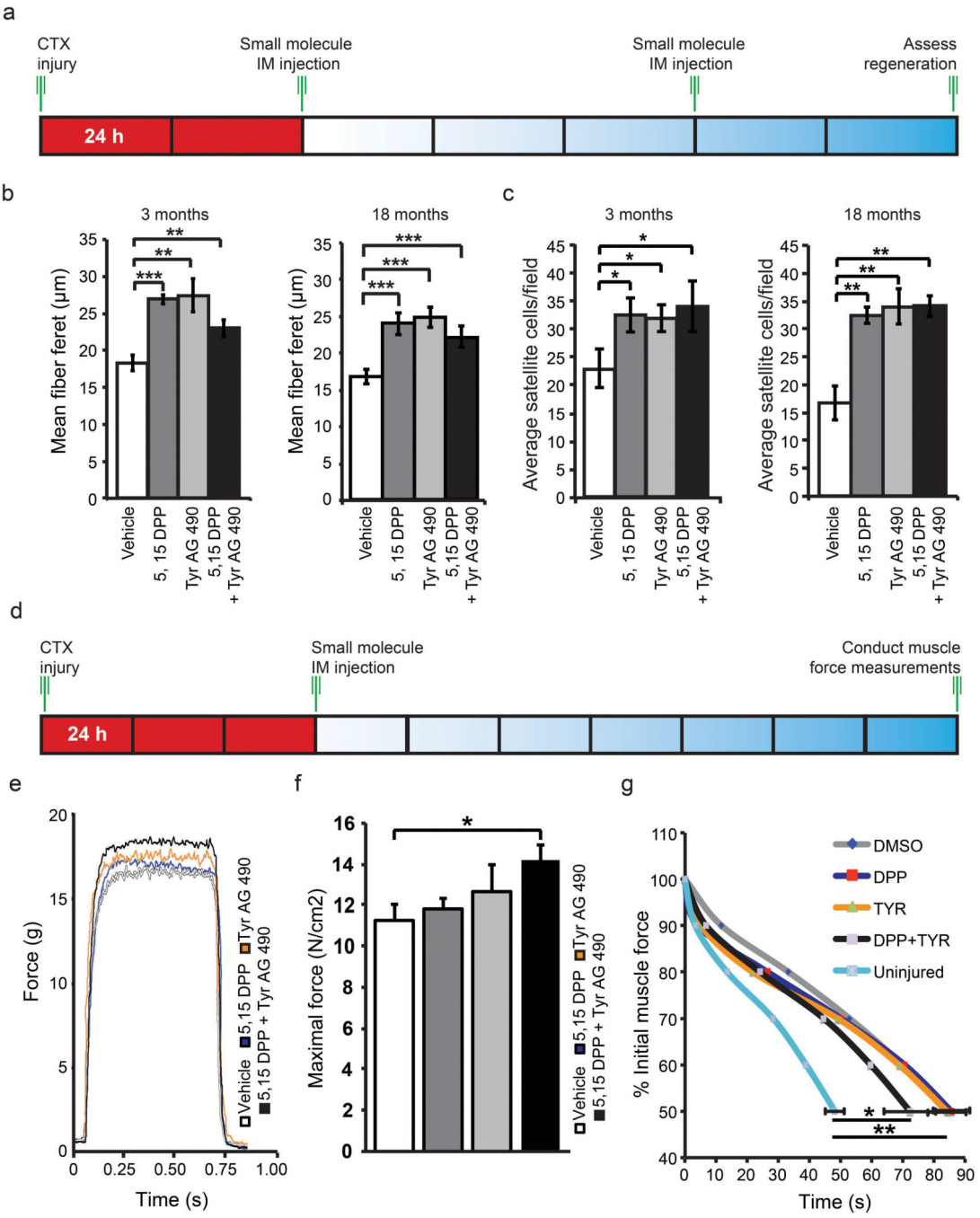

Figure 6.

Direct injection of JAK/STAT inhibitors *in vivo* improves muscle regeneration, increases satellite cell number and functionally improves skeletal muscle. (**a**) Schematic of *in vivo* treatment of regenerating TA muscle with JAK/STAT inhibitors. (**b**) Quantification of the minimal fiber feret following direct IM injection of 5,15 DPP, TyrAG 490 and a combination of both inhibitors into regenerating young adult and older adult TA muscle Data represent the mean ± SEM, *n=4*. ** *p value < 0.01* and *** *p value < 0.001*. (**c**) Quantification of total satellite cells in regenerating young adult or older adult TA muscle

following treatment with JAK/STAT signaling inhibitors. Data represent the mean ± SEM, *n=4*. * $p < 0.05$, ** $p < 0.01$. (**d**) Schematic of *in vivo* treatment of regenerating young adult EDL muscle with JAK/STAT inhibitors and subsequent isolation for functional analysis. (**e**) Force versus Time plots of EDL muscle treated with either vehicle, 5,15 DPP, Tyr AG 490 or a combination of both inhibitors. (**f**) Quantification of the maximal force determined from EDL muscle treated with JAK/STAT inhibitors. (**g**) Fatigue curves indicating the change in % initial muscle force following treatment with JAK/STAT inhibitors. Vehicle (*n=7*) 5,15 DPP (*n=6*), Tyr AG 490 (*n=6*) or a combination of both inhibitors (*n=6*). * $p < 0.05$.